

# Toward Radiation-Magnetohydrodynamic Simulations in Core-Collapse Supernovae

Kei Kotake, Naofumi Ohnishi<sup>†</sup>, Shoichi Yamada<sup>‡</sup>, and Katsuhiko Sato<sup>★</sup>

Science & Engineering, Waseda University, 3-4-1 Okubo, Shinjuku, Tokyo, 169-8555, Japan

<sup>†</sup>Department of Aerospace Engineering, Tohoku University, 6-6-01 Aramaki-Aza-Aoba, Aoba-ku, Sendai, 980-8579, Japan

<sup>‡</sup>Advanced Research Institute for Science and Engineering, Waseda University, 3-4-1 Okubo, Shinjuku, Tokyo, 169-8555, Japan

<sup>★</sup> Department of Physics, School of Science, the University of Tokyo, 7-3-1 Hongo, Bunkyo-ku, Tokyo 113-0033, Japan

**Abstract.** We report a current status of our radiation-magnetohydrodynamic code for the study of core-collapse supernovae. In this contribution, we discuss the accuracy of our newly developed numerical code by presenting the test problem in a static background model. We also present the application to the spherically symmetric core-collapse simulations. Since close comparison with the previously published models is made, we are now applying it for the study of magnetorotational core-collapse supernovae.

## 1. Introduction

Recently, multidimensional studies and simulations of core-collapse supernovae have come into blossom again since 1990's, when the direct observations of global asymmetry in SN 1987A were reported. This trend may be partly because spherically symmetric supernova simulations have not yet produced explosions (e.g., [1]) albeit with the sophistication of the neutrino-transport method including the state-of-the-art nuclear physics, and the detailed weak interaction rates. Meanwhile, there have been the accumulating observations after SN 1987A implying that the core-collapse supernovae are generally aspherical (e.g., [2]). The degree of asymmetry also rises as a function of time, which has been interpreted as an evidence that the inner portion of the explosion are strongly aspherical.

A leap beyond the spherical models seems indeed meaningful, because asphericities in the supernova core should have influence on the nucleosynthesis, neutrino and gravitational-wave emissions [3]. Before the advent of the observations using neutrinos and gravitational waves as new eyes, one hopes to clarify the explosion mechanism of aspherical supernovae.

So far, many physical ingredients to produce aspherical explosion have been investigated, such as convection, possible density inhomogeneities formed prior to core-collapse, rotation and magnetic fields [4] (see [3] for a collective reference), more recently standing shock instability [5] and the excitations of g-modes in the protoneutron star [6]. Whatsoever the origin of the asphericity, the neutrino heating mechanism should play a key role to drive explosions. Thus multidimensional neutrino transport simulations are indispensable. In this contribution, we report the current status of our radiation transport calculations.

## 2. Basic equations of radiation-magnetohydrodynamics

Magnetohydrodynamic (MHD) equations including the neutrino-matter coupling read,

$$\rho \frac{d\mathbf{v}}{dt} + \nabla p + \rho \nabla \Phi - \frac{1}{4\pi} (\nabla \times \mathbf{B}) \times \mathbf{B} = S_M, \quad (1)$$

$$\rho \frac{d\left(\frac{e}{\rho}\right)}{dt} + p \nabla \cdot \mathbf{v} = S_E, \quad (2)$$

$$\frac{dY_e}{dt} = S_{Y_e}. \quad (3)$$

The left-hand side of the above equations is MHD evolution equations, which we numerically integrate by the Newtonian explicit code ZEUS2D [7]. Equation (1) is the Euler equation, where  $\rho$  is the mass density,  $d/dt$  is the Lagrange derivative,  $\mathbf{v}$  is the fluid velocity,  $p$  is the matter pressure,  $\mathbf{B}$  is the magnetic fields solved by the induction equation :  $\partial \mathbf{B} / \partial t = \nabla \times (\mathbf{v} \times \mathbf{B})$  keeping the field divergence-free ( $\nabla \cdot \mathbf{B} = 0$ ) using the CT scheme,  $\Phi$  is the gravitational potential including the general relativistic correction. Equation (2) and (3) expresses the evolution of specific internal energy ( $e$ ) and electron fraction ( $Y_e$ ), respectively. As for the equation of state, we incorporate a tabulated one based on relativistic mean field theory [8].

The right-hand side of the above equations expresses the transfer of momentum ( $S_M$ ), exchange of energy ( $S_E$ ) from neutrinos to matter, and the change of electric charge ( $S_{Y_e}$ ). As for the neutrino reactions, we include the so-called standard set denoted in table 1 in [9], plus nucleon bremsstrahlung [10]. Corrections to the standard neutrino opacities, such as the detailed reaction kinematics of nucleon thermal motions, recoil, and weak magnetism, pair-annihilation/creations among different neutrino flavors, the quenching of the coupling constant above nuclear density, and the modified electron capture rates to the nuclei in the excitation states and so on (see [11]), we omit them for simplicity in the simulation presented here. To determine the right-hand side of the above equations, one has to know the neutrino distribution function  $f(t, \mathbf{r}, \mathbf{p})$  by solving the Boltzmann equation with the collisional terms including the above neutrino reactions in its right-hand side. Fully angle-dependent solutions in multidimensional models (even in 2D) are computationally prohibitive, we employ the flux limited diffusion approximation to relate the first and zeroth angular moment of the neutrino distribution function,

$$\boldsymbol{\psi}_1 = \begin{pmatrix} \psi_{1,r} \\ \psi_{1,\theta} \end{pmatrix} = -\boldsymbol{\Lambda} \cdot [\nabla \psi_0 - \mathbf{A}_1 \psi_0 - \mathbf{C}_1], \quad (4)$$

where  $\psi_0$  and  $\boldsymbol{\psi}_1$  is the zeroth and first angular moment of the neutrino distribution function, respectively. See equation (A25) in [9] for the definition of  $\mathbf{A}_1$  and  $\mathbf{C}_1$ . Here  $\boldsymbol{\Lambda}$  is a flux limiter generalized to 2D as follows,

$$\boldsymbol{\Lambda} = \begin{pmatrix} \Lambda_r & 0 \\ 0 & \Lambda_\theta \end{pmatrix}, \quad (5)$$

whose components are given by  $\Lambda_r = (3\lambda^t)/(3 + \lambda^t |\nabla_r \psi_0| / \psi_0)$ , and  $\Lambda_\theta = (3\lambda^t)/(3 + \lambda^t |\nabla_\theta \psi_0| / \psi_0)$ , where  $\lambda^t$  is the transport mean free path (see Equation (A26) in [9]),  $\nabla_r$  and  $\nabla_\theta$  represents  $\partial/\partial r$  and  $\partial/(r\partial\theta)$ , respectively. With equation (4), one can determine  $\psi_0$  by solving the following zeroth angular moment equation of Boltzmann equation,

$$\frac{1}{c} \frac{d}{dt} \psi_0 + \nabla \cdot \boldsymbol{\psi}_1 + \frac{1}{c} \nabla \cdot \mathbf{v} \omega \frac{\partial}{\partial \omega} \psi_0 = j(1 - \psi_0) - \frac{\psi_0}{\lambda^a} + A_0 \psi_0 + \mathbf{B}_0 \cdot \boldsymbol{\psi}_1 + C_0, \quad (6)$$

which is often referred to as a multi-group flux limited diffusion (MGFLD) equation for neutrinos (again see appendix A in [9] for the definition of unmentioned variables). For the time evolution

of transport, we solve the neutrino-matter coupling (equations (2) (the  $p\nabla \cdot \mathbf{v}$  term is treated in an operator-splitting fashion), (3), and (6) implicitly with performing the Newton Raphson iteration until  $\delta\psi_0$ ,  $\delta Y_e$ , and  $\delta(e/\rho)$  converges to a certain value. More details for the numerical implementation of our code will be presented in the forthcoming paper.

### 3. Static background

Before we apply the newly developed code to the magnetized and rotating supernova simulations, we need to verify the accuracy by the test calculations. Taking the profiles of the density, temperature, and the electron fraction from Bruenn’s 1D model after core bounce [12] as a background, we calculate the neutrino distribution functions of each species ( $\nu_e, \bar{\nu}_e, \nu_x, \bar{\nu}_x$ ) by our 2D computations and compare them with the ones obtained in 1D simulation [12]. We use the 16 energy mesh points which is logarithmically uniform and covers 0.95 - 255 MeV. In Figure 1, the distribution functions of  $\bar{\nu}_e$  and  $\nu_x$  at each energy bin as a function of radius is shown. One can see the good agreement with each other, except for the small discrepancies at  $\sim 20$  km for the lower energy bins. This is also the case for the electron neutrinos, which is not presented here. This may be mainly due to the difference of the numerical implementation of the neutrino transport, and of the employed equation of state. Since close comparison is made in the static background computation, we move on to apply the code to dynamical models.

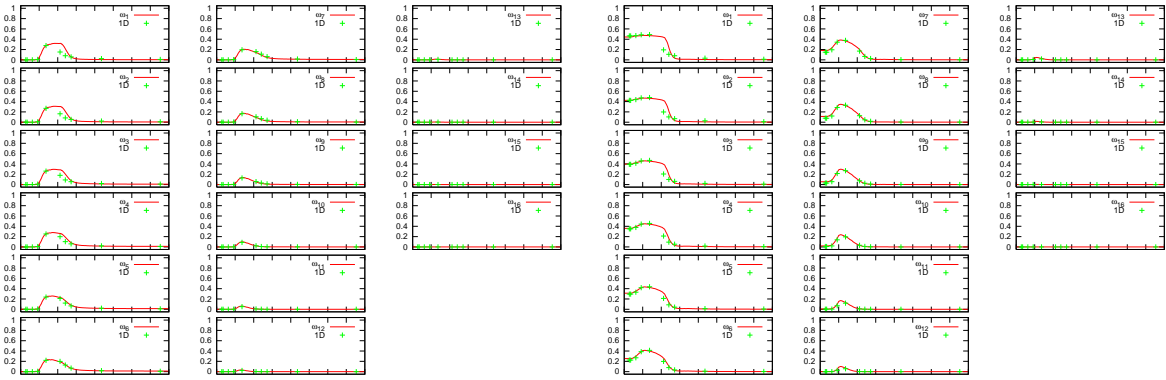


**Figure 1.** Anti-electron (left) and mu-tau (right) neutrino distribution functions at each energy bin as a function of the stellar radius (from 0 to 80 km, equidistantly plotted). Note in the figure that  $\omega_i (i = 1, 16)$  represents the neutrino energy group and that “1D” represents the results by [12].

### 4. Spherically symmetric simulation

Here we examine the accuracy of our code by the spherically symmetric core-collapse simulations of  $15 M_\odot$  progenitor star (Woosley & Weaver 1995). In Figure 2, the velocity (top right), entropy (bottom left),  $Y_e$  (bottom right) distributions at 10 msec after bounce with the evolution of  $Y_e$  up to  $\sim 40$  msec after bounce (top left), are shown. The global profiles are well in good agreement with the previous spherically symmetric calculations [1]. Discrepancies with other calculations could be originated from the differences of employed microphysics, numerical treatment of neutrino transport, general relativistic effects, which seem rather common from models to models [1]. More details about the tests of our newly developed code will be presented soon in elsewhere, with its applications to the magnetorotational core-collapse simulations of massive stars.

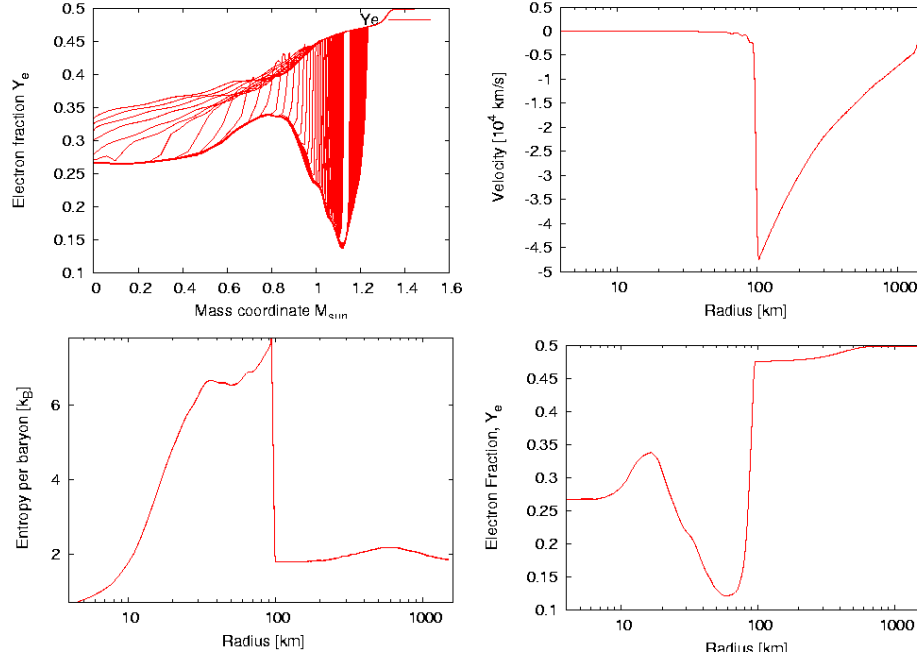


**Figure 2.** Top left panel is the time evolution of  $Y_e$  up to  $\sim 40$  msec after bounce (small blank is due to the data loss). Top right, bottom left, bottom right shows the velocity, entropy,  $Y_e$  distribution at 10 msec after bounce. Compare panels (a), (c), (d) in Figure 20 in [13].

## 5. Outlook

Although  $O(v/c)$  terms in the transport equations, which are one of the most important ingredients for determining the failure or success of the explosion [11], are neglected in the current simulations, we are now implementing them, simultaneously running the MHD collapse models without to see the difference. It is better to employ more detailed neutrino microphysics. Steady progresses with the parallelization of the code are made to test the predictions in our earlier works.

## Acknowledgments

This work was supported in part by the Japan Society for Promotion of Science (JSPS) Research Fellowships (K.K) and a Grant-in-Aid for Scientific Research from the Ministry of Education, Science and Culture of Japan through No.S 14102004, No. 14079202, and No. 14740166.

## 6. References

- [1] Rampp M and Janka H T 2000 *Astrophys. J.* **539** L33, Liebendörfer M *et al* 2005 *Astrophys. J.* **620** 840, Sumiyoshi K *et al* 2005 *Astrophys. J.* in press
- [2] Wang L *et al* 2002 *Astrophys. J.* **579** 671
- [3] Kotake K *et al* 2005 submitted to *Reports on Progress in Physics*
- [4] Obergaulinger M *et al* submitted to *A & A*
- [5] Blondin J M and Mezzacappa A 2005 submitted to *Astrophys. J.*, Ohnishi N, Kotake K, and Yamada S 2005 submitted to *Astrophys. J.*, Foglizzo T, Scheck L, Janka H T 2005 submitted to *A & A*
- [6] Burrows A *et al* 2005 submitted to *Astrophys. J.*
- [7] Stone, J. M. & Norman, M. L. 1992, *Astrophys. J. Suppl.* **80**, 753
- [8] Shen H *et al* 1998 *Nuc. Phys. A* **637** 435
- [9] Bruenn S W 1985 *Astrophys. J. Suppl.* **58** 771
- [10] Hannestad S and Raffelt G 1998 *Astrophys. J.* **507** 339
- [11] Buras R *et al* 2005 *A & A* in press

- [12] Bruenn, S. W. 1992, in Nuclear Physics in the Universe (Philadelphia: Institute of Physics Pub.)
- [13] Liebendörfer M *et al* 2004 *Astrophys. J. Suppl.* **150** 263